EPJ manuscript No.
(will be inserted by the editor)

Quantum vibrational dynamics of the Ar_2ICl cluster

Álvaro Valdés[1] and Rita Prosmiti[2]

[1] Departamento de Física, Universidad Nacional de Colombia, Calle 26, Cra 39, Edificio 404, Bogotá, Colombia
[2] Instituto de Física Fundamental (IFF-CSIC), CSIC, Serrano 123, 28006 Madrid, Spain

Received: date / Revised version: date

Abstract. Quantum mechanical multiconfiguration time-dependent Hartree (MCTDH) calculations are presented for the Ar_2ICl cluster. The Hamiltonian operator is expressed in satellite coordinates, with its potential term being represented as a sum of the three-body ArICl *ab initio* parameterized interactions plus the Ar–Ar ones. The potential surface shows different type of low-lying minima (global and local), that influence the vibrational dynamics of the system. The vibrational ground state properties and specific vibrationally excited states are obtained from improved relaxation MCTDH calculations employing a large number of basis set functions, especially for the angular part, to achieve convergence. By analyzing the spatial density distributions of the vibrational states we are able to characterize the corresponding states to different isomers, such as tetrahedral, linear, bending type ones. The binding energy of each isomer is also computed, and they contribute to evaluate their relative stability, as well as the importance of the underlying multiple minima of the potential surface.

PACS. PACS-key 36.40.-c – PACS-key 33.20.Tq – PACS-key 31.50.-x

1 Introduction

van der Waals (vdW) clusters, e.g., molecules weakly bound to rare-gas atoms, have attracted considerable attention, both experimentally and theoretically (see Refs. [1–3] and references therein). Experimental techniques such as high-resolution infrared (IR) absorption, Fourier-transform IR, and microwave spectroscopy have provided valuable information on the structure and the vibrational dynamics of these complexes [4,3]. In such weakly bound systems the deviation from harmonic behavior is very large, even in the vibrational ground state. Thus, from the theoretical point of view, it is a challenge to obtain accurate energy level structure for these complexes from the potential energy functions, and to interpret the level structure in terms of the vibrational dynamics involved. For triatomic molecules, e.g., dihalogen molecule bound to a rare-gas atom, it is now well known the existence of both linear and T-shaped isomers on their ground electronic state. Improvements in the supersonic cooling techniques have enabled experimentalists to measure relative binding energy of different isomers [5,6,4,7], while with the developments in the *ab initio* electronic structure technology, it became possible to reliably calculate the ground electronic state surfaces of the heavier systems. [8–13]

Studies in small clusters allow us to understand in detail molecular processes, such as bond breaking, energy relaxation. Also they could provide benchmark data for checking the validity of future theoretical approaches, and for developing accurate techniques to determine from first principles the properties of intermolecular interactions. In turn, these are important for applications to more complex systems such as larger clusters. Earlier and recent experimental data are available for larger vdW clusters, like $He_{n=1-3}I_2$, $Ne_{n=1-6}I/Br_2$, $He/Ne/Ar_2Cl_2$, and $Ne_{n=1-5}ICl$ [14–19], and just recently theoretical studies have been also carried out for higher-order He-homonuclear and heteronuclear dihalogen complexes like He_nBr_2,He_nICl, and He_nI_2 with n up to 4 and 38, respectively. [20–25] By increasing the cluster size the difficulties for the theoretical studies increase dramatically, due to the limitations in both electronic and nuclear quantum calculations. However, here for the Ar_2ICl cluster, we take advantage of the availability of triatomic potential energy surface (PES) for the ArICl [10], and their ability to represent the PESs of larger clusters [20,24], as well as the efficiency of the multiconfiguration time dependent Hartree (MCTDH) method [27,28] to handle the computational cost and anharmonic quantum effects of such vdW system. As it may be expected, for the triatomic ArICl cluster the linear isomer is significantly more stable than the near T-shaped and antilinear ones [10]. Although, as we will discuss below when a second Ar atom is included in the cluster then the topology of its PES mainly depends on the balance of the linear, T-shaped, and antilinear ArICl potential interactions with the Ar-Ar ones, and to distinguish on the structure and stability of the Ar_2ICl conformers quantum zero-point energy effects should be considered. Therefore,

Send offprint requests to: avluxan@gmail.com

the plan of this paper is as follows. In section 2 a brief summary of the method used and computational details for calculating the energy levels are provided; the results obtained are presented in section 3, while section 4 summarizes our conclusions.

2 Methodology and computational details

The present calculations were performed using the Heidelberg MCTHD package of codes. [26] The MCTDH method [27, 28] is a general algorithm [26] for solving the time-dependent Schrödinger equation. Briefly, the basis of the MCTDH scheme is that the wavefunction is expanded in a sum of products of time-dependent basis of so-called single-particle functions (SPFs),

$$\Psi(Q_1,....,Q_f,t) = \Psi(q_1,...q_p,t) = \sum_J A_J \Phi_J \qquad (1)$$

where f denotes the number of degrees of freedom and p the number of particles or combined modes. The A_J denotes the MCTDH expansion coefficients with J the composite index $(j_1,....,j_p)$, and the Φ_J denotes a Hartree product or configuration and is a products of SPFs, $\phi(q,t)$. The SPFs are in turn represented by linear combinations of time-independent primitive basis functions or discrete variable representation (DVR) grids. The solution of the MCTDH equations of motion requires the computation of the mean-field matrices at every time step. Thus, for their fast evaluation the Hamiltonian (kinetic and potential terms) is expressed by a sum of products of monoparticle operators (acting only on one particle), the so-called product structure.

To perform the calculation of the ground and vibrationally excited states of the Ar_2ICl complex we use the *improved relaxation* (IR) and *block improved relaxation* (BIR) methods implemented in the Heidelberg MCTDH code [26,27,29,30]. The MCTDH method does not take into account particle exchange symmetry, and thus in the present study all Ar nuclei are treated as distinguishable particles. [28] The Hamiltonian operator and the wavefunction are represented on a grid in the internal satellite coordinates ($\mathbf{r}$,$\mathbf{R_1}$,$\mathbf{R_2}$), with $\mathbf{r}$ being the vector joining the I and Cl atoms, while $\mathbf{R_1}$ and $\mathbf{R_2}$ are the vectors from the center of mass of the ICl molecule to each Ar atom, respectively, θ_1/θ_2 are the polar and φ_1/φ_2 the azimuthal angles associated with the $\mathbf{R_1}/\mathbf{R_2}$ vectors. By choosing the $\mathbf{R_2}$ vector being on the the XZ-plane φ_2 is zero, and the 3 angles with the 3 vectors constitue the vibrational coordinates. In turn, the full-dimensional 6D vibrational Hamiltonian of the Ar_2ICl system can be written as [33]:

$$\hat{H} = -\frac{\hbar^2}{2m}\frac{\partial^2}{\partial r^2} + \frac{\mathbf{j}^2}{2mr^2} + \sum_{k=1}^{2}\left(-\frac{\hbar^2}{2\mu}\frac{\partial^2}{\partial R_k^2} + \frac{\mathbf{l_k^2}}{2\mu R_k^2}\right) - \frac{\hbar^2}{m_{ICl}}\nabla_1\cdot\nabla_2 + V(\mathbf{r},\mathbf{R_1},\mathbf{R_2}), \qquad (2)$$

where $\mathbf{j}$ and $\mathbf{l_k}$ are the angular momenta associated to the vectors $\mathbf{r}$ and $\mathbf{R_k}$, respectively. m is the reduced mass of the diatomic ICl molecule, μ is the reduced mass of the Ar-ICl system and m_{ICl} is the sum of the masses of the I and Cl atoms. The effect of the kinetic energy coupling terms $(-\frac{\hbar^2}{m_{ICl}}\nabla_1\cdot\nabla_2)$ has been estimated to be less than 0.02 cm^{-1} for the ground state and less than 0.5 cm^{-1} for the higher excited vibrational states in this case, and thus, we did not consider this term further on. Also, the same behavior has been found in the vibrational states of the similar vdW molecules [31,32].

For the potential form we employ a sum of the three-body ArICl interactions plus the Ar–Ar interaction. Such analytical expressions have been found to describe very accurately tetra-atomic *ab initio* CCSD(T) potentials of similar type vdW systems [31,32,24], as well as to provide a very detailed description of their lowest vibrational states [33,22] in agreement with the experimental findings [17] for similar type vdW systems. Thus, the $V(\mathbf{r},\mathbf{R_1},\mathbf{R_2})$ form is given by:

$$V(\mathbf{r},\mathbf{R_1},\mathbf{R_2}) = \sum_{k=1,2} V_{ArICl}(\mathbf{r},\mathbf{R_k}) + V_{Ar-Ar}(\mathbf{R_1},\mathbf{R_2}) + U_{ICl}(\mathbf{r}) \qquad (3)$$

where the $V_{ArICl}(\mathbf{r},\mathbf{R_k})$ terms are the CCSD(T) parameterized potential of the ArICl complex from Ref. [10], the $V_{Ar-Ar}(\mathbf{R_1},\mathbf{R_2})$ terms are the potential function for Ar_2 given in Ref. [34], and $U_{ICl}(\mathbf{r})$ is the diatomic interaction ICl potential calculated at the CCSD(T) level of theory from Ref. [33]

The MCTDH program requires the potential energy operator, $V(\mathbf{r},\mathbf{R_1},\mathbf{R_2})$, to be written as the sum of products of single-particle operators. The POTFIT program is used to obtain the desired product representation by expanding the PES in natural potentials [35,36]. In Table 1 we present the parameters used for the POTFIT calculations, together with the primitive basis employed in both POTFIT and the MCTDH calculations. For each degree of freedom we show the corresponding type of basis set used, *HO* stands for the harmonic oscillator *discrete variable representation* (DVR) basis, *Leg* corresponds to the one dimensional Legendre DVR basis, and *exp* is the exponential DVR basis. We should point here that test calculations have shown no effect of the r coordinate on the vdW vibrational states of the ArICl system, thus we finally solved the 5D problem. The number of natural potentials included in the POTFIT calculations for the V_{ArICl} and V_{Ar-Ar} potential energy surfaces are also listed. The introduction of weights can increase the accuracy of the potential fit for the relevant regions, and thus in Table 1 we list the relevant regions of the potential considered in the above mentioned calculations, as well as the root mean square (rms) error for all the fits.

In Table 1 we resume the number of single particle functions (SPFs) included in the *improved relaxation* calculations for Ar_2ICl cluster. In order to obtain a better performance of the calculations, we combine the highly correlated degrees of freedom in the $[R_1,\theta_1]$ and $[R_2,\theta_2]$ modes. The populations of the highest (least populated) natural orbital is included in Table 1. The populations of

Table 1. Primitive basis sets, SPFs, and POTFIT parameters used in the MCTDH IR calculations. Contr indicates the mode over which a contraction is performed.

	ArICl	Ar-Ar
Primitive basis		
$N_{R_{1,2}}$ (HO)	51	51
$R_{1,2}$-range (Å)	[3.18, 6.35]	[3.18, 6.35]
N_θ (Leg)	61	61
θ-range (rad)	[0, π]	[0, π]
N_φ (exp)	-	61
φ-range (rad)	[0, 2π]	[0, 2π]
Natural potentials		
N_{R_1,R_2}	20	-
N_{θ_1,θ_2}	-	Contr
$N_{R_1\theta_1/R_2\theta_2}$	-	Contr/150
N_{φ_1}	-	10
Relevant regions	V < 20 cm^{-1}	V < 100 cm^{-1}
rms error on relevant grid points (cm^{-1})	0.1	1.5
SPFs	Ar_2ICl	
N_{R_1,θ_1}	8	
N_{R_2,θ_2}	8	
N_{φ_1}	12	
Least populated orbital population	1×10^{-4}	

Table 2. Well-depths (D_e in cm^{-1}) and equilibrium distances (in Å and deg) for the indicated configurations of the Ar_2ICl PES.

(#T,#L,#A,#B)	D_e	R^e	$\theta^e(\varphi^e)$
(1,1,0,0)	564.06	3.94/4.05	107/0(0)
(2,0,0,0)	556.98	3.94/3.94	107/107(59)
$(0,1,0,1_1)$	554.74	4.05/4.93	0/52(0)
(0,1,1,0)	522.63	4.05/5.36	0/180(0)
$(1,0,0,1_2)$	476.79	3.94/5.25	107/154(0)

the highest (least populated) natural orbital is included in Table 1. The improved relaxation runs are converged to within 10^{-4} cm^{-1}. In the BIR calculations we employ (22,22,16) single-particle functions (SPFs) for the ($[R_1,\theta_1]$,$[R_2,\theta_2]$,φ_1) modes, respectively, to calculate 40 vibrationally excited states. The convergence to the states is getting more difficult as the excitation energy increases, that implies higher density of states, and/or the degree of the state degeneracy.

3 Results

In Fig. 1 we display low-lying minima configurations of the Ar_2ICl PES (see Eq. 3), while in Table 2 their well-depths and equilibrium values are listed. We use the label (#T,#L,#A,#B), where #T, #L, #A and #B denotes the number of Ar atoms in the near T-shaped ($\theta_{1/2}$=107°), linear ($\theta_{1/2}$=0°), anti-linear ($\theta_{1/2}$=180°), and bending ($\theta_{1/2}$=52°, namely B_1, or 154°, namely B_2) configurations (see Fig. 1). The (1,1,0,0) structure at energy of - 564.1 cm^{-1} is the global minimum, while the other ones corresponding to (2,0,0,0), $(0,1,0,1_1)$, (0,1,1,0) and $(1,0,0,1_2)$ configurations are local minima of the PES at higher energies, above the global minimum by 7.1, 9.4, 41.5, and 87.3 cm^{-1}, respectively. The global and the lowest two local minima are quite close in energy, within less than 10 cm^{-1}, while the linear arrangements of all atoms is higher in energy due to the stronger Ar–Ar interaction compared to the Ar–ICl ones. We should also point out that various other stationary points are located on the surface, corresponding to saddle points that connect symmetric minima, such as the (0,2,0,0) one, although we only discuss here the minima structures that, as we will see later on, influence the vibrational dynamics of the cluster. Fig. 2 shows 1D representations of the Ar_2ICl PES, where the minimun energy paths are plotted as a function of the θ_1 angle for planar configurations with ArICl being linear (see top panel), and θ_1 and φ_1 for non-planar configurations with ArICl being near-T-shaped (θ_2=107°, φ_1=59° and $\theta_1 = \theta_2$=107°, see middle and bottom panels, respectively). One can also see the different minima on the PES, as well as the barriers between them. In the top panel the (0,2,0,0) barrier at energy of -429.2 cm^{-1} connects the two symmetric $(0,1,0,1_1)$ minima, the barriers between $(0,1,0,1_1) \leftrightarrow (1,1,0,0) \leftrightarrow (0,1,1,0)$ are found at -480.9 and -470.3cm^{-1}, respectively, while in the middle panel the barriers between $(1,1,0,0) \leftrightarrow (2,0,0,0) \leftrightarrow (1,0,0,1_2)$ are shown around -422 and -467cm^{-1}, respectively.

In turn, we employ the analytical PES to carry out quantum dynamics calculation using the MCTDH approach. In a first step we carried out BIR calculations including a block of 40 initial states. However we should point out that due to the degeneracy of the states the density of states becomes high, and convergence problems appeared. In this way we achieved convergence for only 12 of the lowest vibrational states, as the BIR calculation required more computational resources. Thus, we used the IR method to converge specific vibrational levels of the Ar_2ICl cluster lying higher in energy. We should note that a large number of angular functions (see Table 1) are needed for achieving convergence in these computations. For the generation of the initial guess in the IR calculations we choose the initial wavefunction by solving different reduced dimensional model Hamiltonians, that could provide initial states with a reasonable overlap with the eigenstate of interest. In this way we generate a convenient initial guess for each state accelerating the relaxation process for achieving convergence.

In Table 3 we list the number of states and their corresponding energies comparing them with data available in the literature, [20] as well as their assignment, if any, to each isomer of the Ar_2ICl cluster. We also follow the (#T,#L,#A,#B) notation, as it has been described above, to characterize the vibrational states. One can see that both calculations predict that the (1,1,0,0) isomer to be the most stable one, however we can see a difference in its binding energy of 5.13 cm^{-1} mainly due to the limitations in the number of the angular basis set functions in the pre-

Table 3. Vibrational energies (in cm^{-1}) for the indicated Ar_2ICl states from the MCTDH calculations, and comparison with previously reported values.

No Level	Energy	Assigned
n=0,1	-489.63(-484.5)[a]	(1,1,0,0)
n=2,3	-483.65(-469.9)[a]	(2,0,0,0)
n=4,5	-483.52	$(0,1,0,1_1)$
n=6,7	-478.29(-472.5)[a]	$(1,1,0,0)\nu_{(\theta 2,\varphi_1)}=1$
n=8,9	-467.49	$(1,1,0,0)\nu_{\varphi_1}=1$
n=10,11	-466.93	$(1,1,0,0)\nu_{(\theta 2,\varphi_1)}=2$
–	-451.34	(0,1,1,0)
–	-416.80	$(1,0,0,1_2)$

[a] Results from previous variational quantum calculations[20].

vious variational calculations [20]. Such convergence problems also affect the other 2 states reported by the previous variational calculations (see Table 3). In the present calculations, the next isomers correspond to the (2,0,0,0) and $(0,1,0,1_1)$ at energy of -483.65 and -483.52 cm^{-1}, that are less stable than the (1,1,0,0) one by just only 6 cm^{-1}, while the (0,1,1,0) and $(1,0,0,1_2)$ ones are lying higher than the (1,1,0,0) isomer by 38 and 73 cm^{-1}, respectively. In Fig. 2 we show the 1D averaged angular probability distributions along θ_1 and φ_1 coordinates for the indicated eigenstates, together with the underlying minimum energy paths of the PES in the same coordinates. The zero probability density for each state is shifted to its energy value (see Table 3). One can clearly see that the peaks of the wavefunction probability are around the corresponding potential wells, as well as their relative energy order and stability. We should also note (see bottom panel of Fig. 2) the degeneracy of the (2,0,0,0) state due to the symmetry of the PES, as both n=2 and n=3 states (see Table 3) are shown. The 3D probability distributions in the Cartesian coordinates (Z,X) or (X,Y) of the ground and indicated excited vibrational states are displayed in Figs. 3 and 4, respectively. For these plots the ArICl complex is kept fixed at its linear configuration with the second Ar atom moving in the ZX-plane (see Fig. 3, upper-middle and bottom panels of Fig. 4) or with ArICl at its near T-shaped configuration and the remainder Ar atom moving in XY-plane (see top panel of Fig. 4) or ZX-plane (see lower-middle panel of Fig. 4). The ground state conformer has one Ar atom in each of the near T-shaped and linear wells (see Fig. 3), while the distribution probabilities for the others show localization of the corresponding the wavefunctions at different potential wells, in consistency with the 1D angular distributions (see Fig. 2), and the assignment given in Table 3.

Experimental measurements are available for similar vdW complexes, such as He_2Br_2 and He_2ICl, from recent laser-induced fluorescence (LIF) and two-laser action spectroscopic studies [17,19], where only the (1,1,0,0) and (2,0,0,0) isomers have been stabilized. Further, based on the sum of the experimental binding energies of the triatomic complexes, the (1,1,0,0) isomer has been estimated to be more stable than the (2,0,0,0) one [17]. Unfortunately, no further experimental data are yet available for complexes with heavier rare-gas atoms, such as Ar_2ICl, for guiding us to establish general trends in the relative stability of the multiple isomers of these vdW clusters. However, we have shown that the isomers are somehow relating with the properties of their triatomic rare-gas-dihalogen counterparts, the energetic balance between them, as well as the interaction between the rare-gas atoms.

4 Summary

The structures and stabilization energetics of different conformers of the Ar_2ICl vdW cluster were characterized and determined in the present study. The full interaction between the ICl molecule and the Ar atoms is approximated by a sum of three- and two-body potential scheme, employing analytical ArICl and Ar_2 potential forms, that have been parameterized to *ab initio* calculations. The potential energy surface shows high anisotropy with multiple and close-lying in energy minima, *e.g.* the global and the two lowest local minima are within just 10 cm^{-1}. Quantum vibrational bound state calculations were performed using the MCTDH method. The POTFIT algorithm was used to expand the PES in product form, while a mode combinations scheme was employed to accelerate the relaxation process using a large number of basis set functions in order to achieve convergence. Binding energies and probability density distributions were computed for the ground and specific vibrationally excited vdW states. It was found that the ground state (1,1,0,0) isomer is localized in the global potential well, while the other less stable ones are localized in local potential minima lying higher in energy. The binding energies of the three most stable isomers are very close in energy within 6 cm^{-1}, while the values for the two remaining ones are higher by 38 and 72 cm^{-1} then the energy value of the most stable (1,1,0,0) isomer. Although, the results presented here on the structure and energetics of the Ar_2ICl vdW cluster are the most detailed description of these isomers, their accuracy is still limited to the uncertainties of the underlying potential surface, and further experimental studies are demanded in order to assert our prediction on such heavier vdW systems.

Acknowledgments

The authors thank to Centro de Calculo del IFF, and SGAI (CSIC) for allocation of computer time. This work has been supported by MICINN grant No. FIS2011-29596-C02-01, MINECO grant No. FIS2014-51933-P, COST Actions CM1204 (XLIC) and CM1405(MOLIM), and by the Research Headquarters Address Bogota - DIEB, National University of Colombia, QUIPU code 201010023374, HERMES code: 27008.

Author contribution statement

All authors contributed equally to the paper.

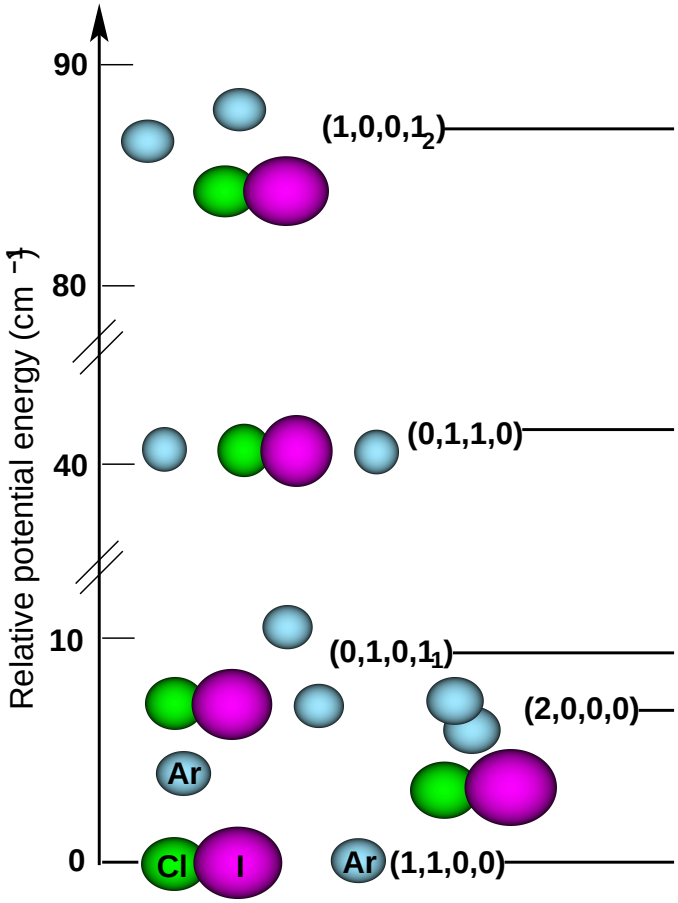

Fig. 1. Configuration of the global and local Ar_2ICl potential minima and their relative potential energy values.

References

1. A. Rohrbacher, N. Halberstadt, K.C. Janda, Ann. Rev. Phys. Chem. **51**, 405 (2000).
2. D. Bonhommeau, N. Halberstadt, U. Buck, Inter. Rev. Phys. Chem. **26**, 353 (2007).
3. J.A. Beswick, N. Halberstadt, K.C. Janda, Chem. Phys. **399**, 4 (2012).
4. D. S. Boucher, R. A. Loomis, *Stabilization of Different Conformers of Weakly Bound Complexes to Access Varying Excited-State Intermolecular Dynamics* (John Wiley & Sons, Inc. 2008) 375–419.
5. D. S. Boucher, J.P. Darr, M.D. Bradke, R. A. Loomis, A.B. McCoy, Phys. Chem. Chem. Phys. **6**, 5275 (2004).
6. S. E. Ray, A. B. McCoy, J. J. Glennon, J. P. Darr, E. J. Fesser, J. R. Lancaster, R. A. Loomis, J. Chem. Phys. **125**, 164314 (2006).
7. Y. Zhang, K. Vidma, D.H. Parker, R. A. Loomis, J. Chem. Phys. **130**, 104302 (2009).
8. R. Prosmiti, C. Cunha, P. Villarreal, G. Delgado-Barrio, J. Chem. Phys. **117**, 7017 (2002).
9. R. Prosmiti, P. Villarreal, G. Delgado-Barrio, Chem. Phys. Lett. **359**, 473 (2002).
10. A. Valdés, R. Prosmiti, P. Villarreal, G. Delgado-Barrio, Chem. Phys. Lett. **357**, 328 (2003).
11. L. Garcia-Gutierrez, L. Delgado-Tellez, Á. Valdés, R. Prosmiti, P. Villarreal, G. Delgado-Barrio. J. Phys. Chem. A **113**, 5754 (2009).
12. C. Sanz-Sanz, O. Roncero, R. Hernández-Lamoneda, J. M. Pio, M. A. Taylor, K. C. Janda, J. Chem. Phys. **132**, 221103 (2010).
13. L. Delgado-Tellez, A. Valdés, R. Prosmiti, P. Villarreal, G. Delgado-Barrio, J. Chem. Phys. **134**, 214304 (2011).
14. J.A. Blazy, B.M. DeKoven, T.D. Russell, D.H. Levy, J. Chem. Phys. **72**, 2439 (1980).
15. J. C. Drobits, M. I. Lester, J. Chem. Phys. **86**, 1662 (1987).
16. M. Gutmann, D. M. Willberg, A. H. Zewail, J. Chem. Phys. **97**, 8048 (1992).
17. D.S. Boucher, J.P. Darr, D.B. Strasfeld, R.A. Loomis, J. Phys. Chem. A **112**, 13393 (2008).
18. J.M. Pio, M.A. Taylor, W.E. van der Veer, C.R. Beiler, J.A. Cabrera, K.C. Janda, J. Chem. Phys. **133**, 014305 (2010).
19. J. P. Darr, R. A. Loomis. Chem. Phys. Lett. **586**, 34 (2013).
20. C. Diez-Pardos, A. Valdés, R. Prosmiti, P. Villarreal P, G. Delgado-Barrio, Theor. Chem. Acc. **118**, 511 (2007).
21. Á. Valdés, R. Prosmiti, P. Villarreal, G. Delgado-Barrio, J. Phys. Chem. A **116**, 7169 (2012).
22. Á. Valdés, R. Prosmiti, J. Phys. Chem. A **117**, 7217 (2013).
23. P. M. Felker, J. Chem. Phys. **125**, 184313 (2006).
24. A. Valdés, P. Barragán, R. Pérez de Tudela, J. S. Medina, L. Delgado-Tellez, R. Prosmiti, Chem. Phys. **399**, 39 (2012).
25. R. Pérez de Tudela, P. Barragán, Á. Valdés, R. Prosmiti, J. Phys. Chem. A **118**, 6492 (2014).

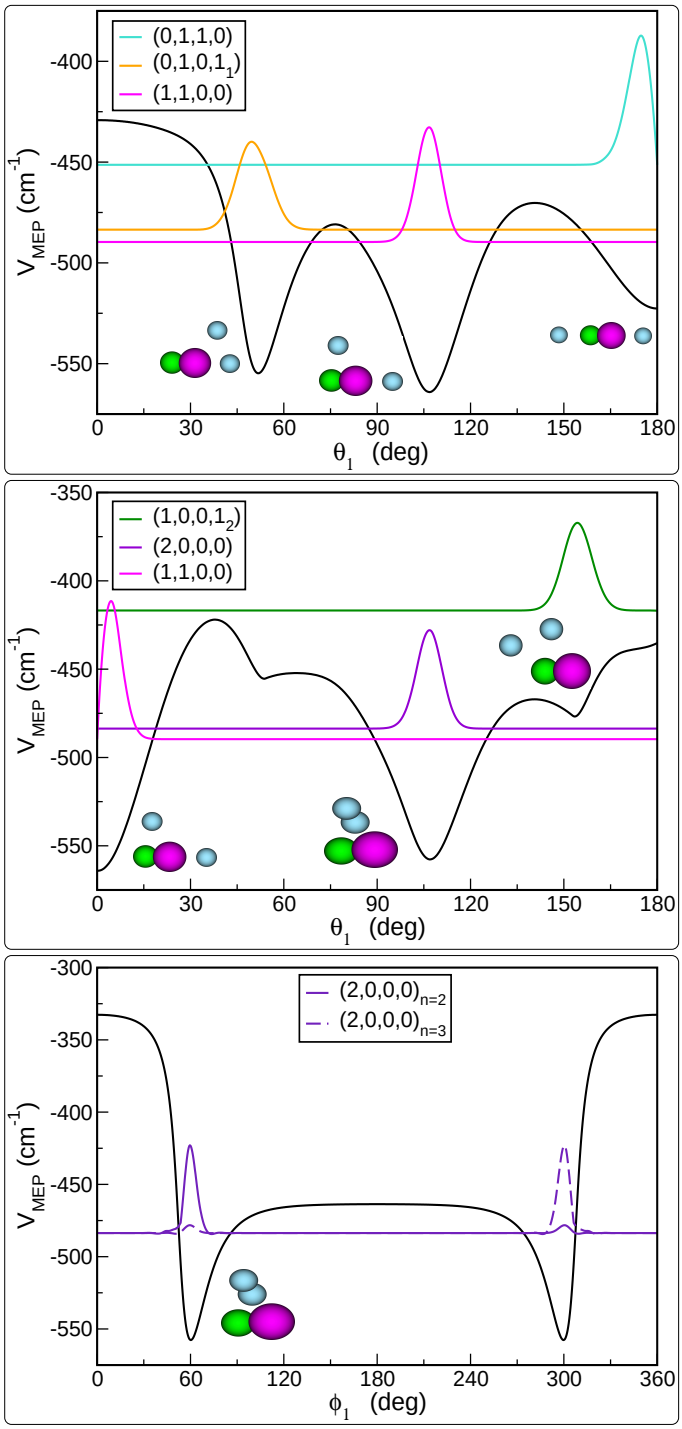

Fig. 2. Minimum energy paths as a function of angle θ_1 for planar configurations with θ_2=0° (top panel), and non-planar with φ_1=59° and θ_2=107° (middle panel) and as a function of φ_1 for non-planar configurations with $\theta_1 = \theta_2$=107° (bottom panel) of the Ar_2ICl cluster (see text). The probability distributions for the ground and lowest excited vibrational states of Ar_2ICl are also shown, with the zero probability being shifted to the energy value of each eigenstate (see Table 3).

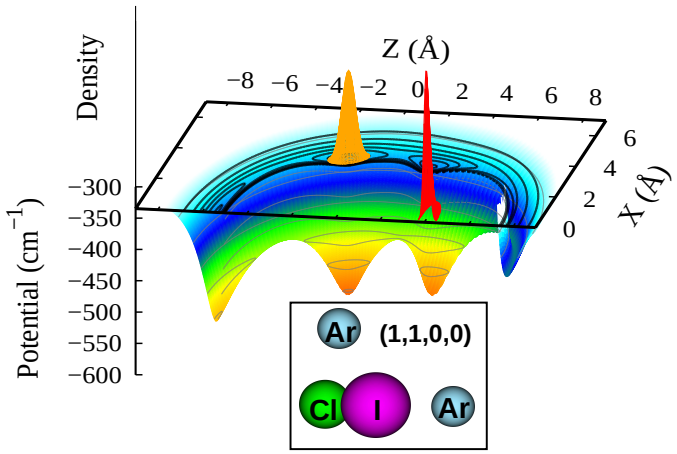

Fig. 3. 3D plot of the probability density distributions of the ground (1,1,0,0) vibrational state of the Ar_2ICl complex, together with the projection of the underlying potential energy surface. For the potential curves the ArICl system is kept at its linear configuration, with the ICl fixed along the Z-axis and its center of mass at the origin of the axis (as in the top panel of Fig. 2), while the second Ar atom is moving in the ZX-plane. In the inset plot the configuration of the global potential minimum is displayed.

26. G. A. Worth, M. H. Beck, A. Jäckle, H.-D. Meyer, The MCTDH Package, Version 8.2, (2000). H.-D. Meyer, Version 8.3 (2002), Version 8.4 (2007). See http://mctdh.uni-hd.de.
27. M. H. Beck, A. Jäckle, G. A. Worth, H.-D. Meyer, Phys. Rep. **324**, 1 (2000).
28. H.-D. Meyer, WIREs Comput. Mol. Sci. **2**, 351 (2012).
29. H.-D. Meyer, F. Le Quéré, C. Léonard, F. Gatti, Chem. Phys. **329**, 179 (2006).
30. L. J. Doriol, F. Gatti, C. Iung, H.-D. Meyer, J. Chem. Phys. **129**, 224109 (2008).
31. Á. Valdés, R. Prosmiti, P. Villarreal, G. Delgado-Barrio, J. Chem. Phys. **122**, 044305 (2005).
32. Á. Valdés, R. Prosmiti, P. Villarreal, G. Delgado-Barrio, J. Chem. Phys. **125**, 014313 (2006).
33. Á. Valdés, R. Prosmiti, P. Villarreal, G. Delgado-Barrio, J. Chem. Phys. **135**, 244309 (2011).
34. T. Xiao-Fei, Y. Chuan-Lu, X. Jing, Chin. Phys. B **19**, 123102 (2010).
35. A. Jäckle, H.-D. Meyer, J. Chem. Phys. **104**, 7974 (1996).
36. A. Jäckle, H.-D. Meyer, J. Chem. Phys. **109**, 3772 (1998).

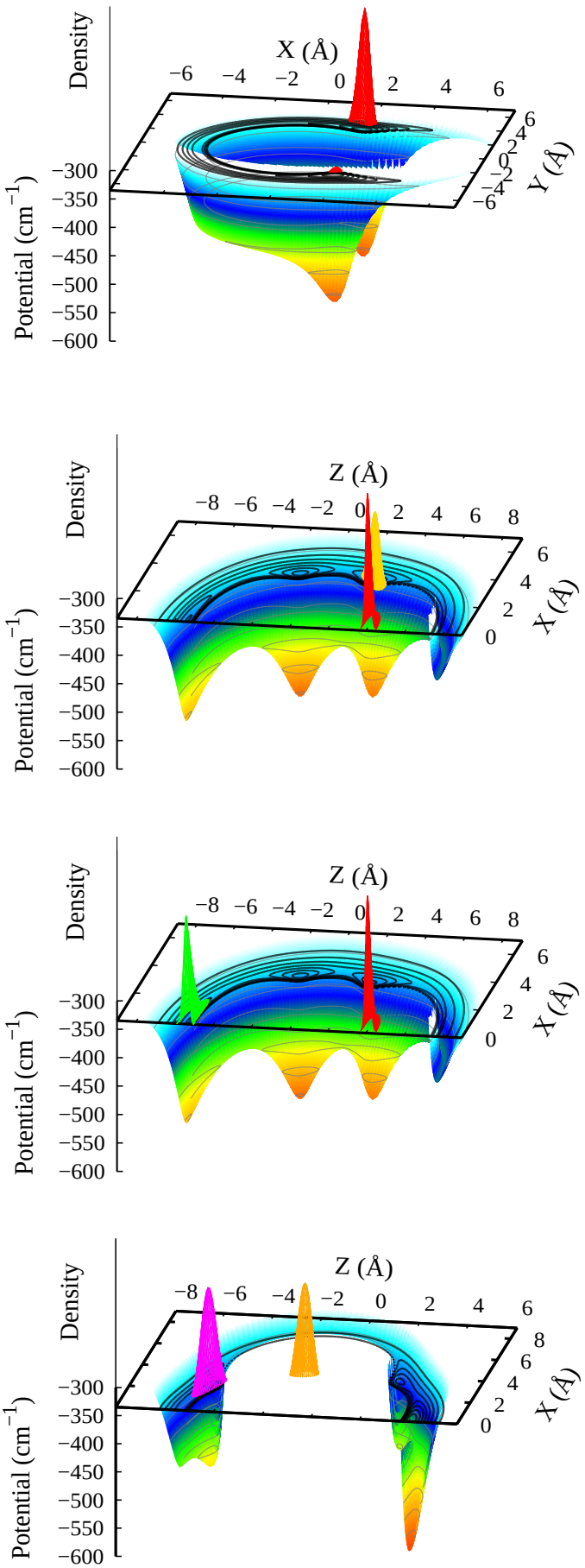

Fig. 4. As in Fig. 3 for the (2,0,0,0), (0,1,0,1_1), (0,1,1,0) and (1,0,0,1_2) (from top to bottom panels) excited vibrational states of the Ar_2ICl complex. For the underlying potential curves the ArICl system is fixed at its linear (along the Z-axis) or near T-shaped configurations, as in the panels of Fig. 2, while the second Ar atom is moving in the ZX-plane or XY-plane, respectively (see text).